

RESEARCH ARTICLE

Genetic and structural analysis of the *in vivo* functional redundancy between murine NANOS2 and NANOS3

Danelle Wright¹, Makoto Kiso² and Yumiko Saga^{1,2,3,*}

ABSTRACT

NANOS2 and NANOS3 are evolutionarily conserved RNA-binding proteins involved in murine germ cell development. NANOS3 is required for protection from apoptosis during migration and gonadal colonization in both sexes, whereas NANOS2 is male-specific and required for the male-type differentiation of germ cells. Ectopic NANOS2 rescues the functions of NANOS3, but NANOS3 cannot rescue NANOS2 function, even though its expression is upregulated in *Nanos2*-null conditions. It is unknown why NANOS3 cannot rescue NANOS2 function and it is unclear whether NANOS3 plays any role in male germ cell differentiation. To address these questions, we made conditional *Nanos3/Nanos2* knockout mice and chimeric mice expressing chimeric NANOS proteins. Conditional double knockout of *Nanos2* and *Nanos3* led to the rapid loss of germ cells, and *in vivo* and *in vitro* experiments revealed that DND1 and NANOS2 binding is dependent on the specific NANOS2 zinc-finger structure. Moreover, murine NANOS3 failed to bind CNOT1, an interactor of NANOS2 at its N-terminal. Collectively, our study suggests that the inability of NANOS3 to rescue NANOS2 function is due to poor DND1 recruitment and CNOT1 binding.

KEY WORDS: Germ cells, Mouse, Nanos, RNA-binding protein

INTRODUCTION

In species that reproduce through sexual reproduction, the development of functional germ cells is essential in order to pass along genetic information to the next generation. RNA-binding proteins play major roles in regulating correct germ cell development (Licatalosi, 2016). These proteins generally make functional complexes; however, what kind of protein structures are needed to form these complexes and bind specific RNA are largely unknown. One family of RNA-binding proteins required for germ cell development is NANOS. There are three NANOS homologues in the mouse: NANOS1 was found to be expressed in the central nervous system, but no phenotype for germ cell development was observed when it was knocked-out (Haraguchi et al., 2003). NANOS3 is expressed in the primordial germ cells (PGCs) to protect them from apoptosis during migration to the future gonad in both sexes, whereas NANOS2 is male specific and needed for male


germ cell differentiation (Suzuki et al., 2007; Tsuda, 2003). These two proteins become expressed again during spermatogenesis, during which NANOS2 is expressed in spermatogonial stem cells and NANOS3 is expressed in later aligned spermatogonia (Lolicato et al., 2008; Sada et al., 2009). NANOS proteins are structurally similar in that they have a conserved zinc-finger (ZF) domain and similar N-terminal. In the case of NANOS2, the ZF domain is needed for interaction with its recently discovered partner, dead end 1 (DND1) (Suzuki et al., 2016). DND1 is an RNA-binding protein conserved among vertebrates that is important for the survival of PGCs and functions in numerous RNA regulatory processes in germ cell development (Gross-Thebing and Raz, 2020). Suzuki et al. previously reported that the loss of DND1 results in the loss of association between NANOS2 and its target RNA (Suzuki et al., 2016). Moreover, they reported that mutation of the CCHC-CCHC motif of the ZF domain prevents DND1 binding. The other key protein domain, the N-terminal, is needed for interaction with the CCR4-NOT deadenylation complex, specifically by binding the component CNOT1 (Suzuki et al., 2014, 2012). NANOS2 directly binds CNOT1, and NANOS2 and DND1 binding is necessary to recruit target RNAs. NANOS2, DND1, CCR4-NOT and other proteins form processing bodies (P-bodies), which are ribonucleoprotein granules for RNA storage and degradation (Eulalio et al., 2007; Kedersha et al., 2005). Currently, the functions and formation mechanisms of P-bodies are unclear (Aizer et al., 2008), and many studies have focused on elucidating their properties among cell types and in comparison with other ribonucleoprotein particle granules such as stress granules (Decker and Parker, 2012; Stoecklin and Kedersha, 2013). In male germ cells, the formation of these specific NANOS2-DND1 P-body-like granules may be essential for male differentiation to proceed.

If *Nanos2* is knocked out, several characteristic phenotypes are observed in the embryonic testes that lead to the eventual sterility of male mice. First, germ cells fail to express DNMT3L, a methyltransferase required for establishing male-type DNA methylation, and other markers for male germ cell differentiation (Suzuki and Saga, 2008). Instead, *Nanos2*-null gonocytes begin to express the normally repressed transcription factor STRA8, by which they abnormally enter meiosis and eventually die owing to apoptosis (Suzuki et al., 2016; Suzuki and Saga, 2008; Tsuda, 2003). Moreover, NANOS3, which is downregulated following the start of NANOS2 expression at around E13.5, becomes highly expressed in the absence of NANOS2 (Suzuki et al., 2007). Of note, although ectopic NANOS2 was reported to rescue the functions of NANOS3 in PGCs in early development, NANOS3 cannot rescue the later NANOS2 function for male differentiation even though it becomes upregulated in *Nanos2*-null germ cells (Tsuda, 2003). However, it is unknown whether NANOS3 plays any role during this sexual differentiation stage in mouse germ cells.

Thus, using conditional *Nanos3/Nanos2* double knockout mice and chimeric mice expressing chimeric NANOS protein constructs

¹Department of Genetics, The Graduate University for Advanced Studies, SOKENDAI, Mishima 411-8540, Japan. ²Department of Gene Function and Phenomics, Mammalian Development Laboratory, National Institute of Genetics, Mishima 411-8540, Japan. ³Department of Biological Sciences, Graduate School of Science, The University of Tokyo, Tokyo 113-0033, Japan.

*Author for correspondence (ysaga@nig.ac.jp)

 D.W., 0000-0002-7954-7193; M.K., 0000-0002-1448-6625; Y.S., 0000-0001-9198-5164

Handling Editor: Haruhiko Koseki

Received 22 April 2020; Accepted 4 November 2020

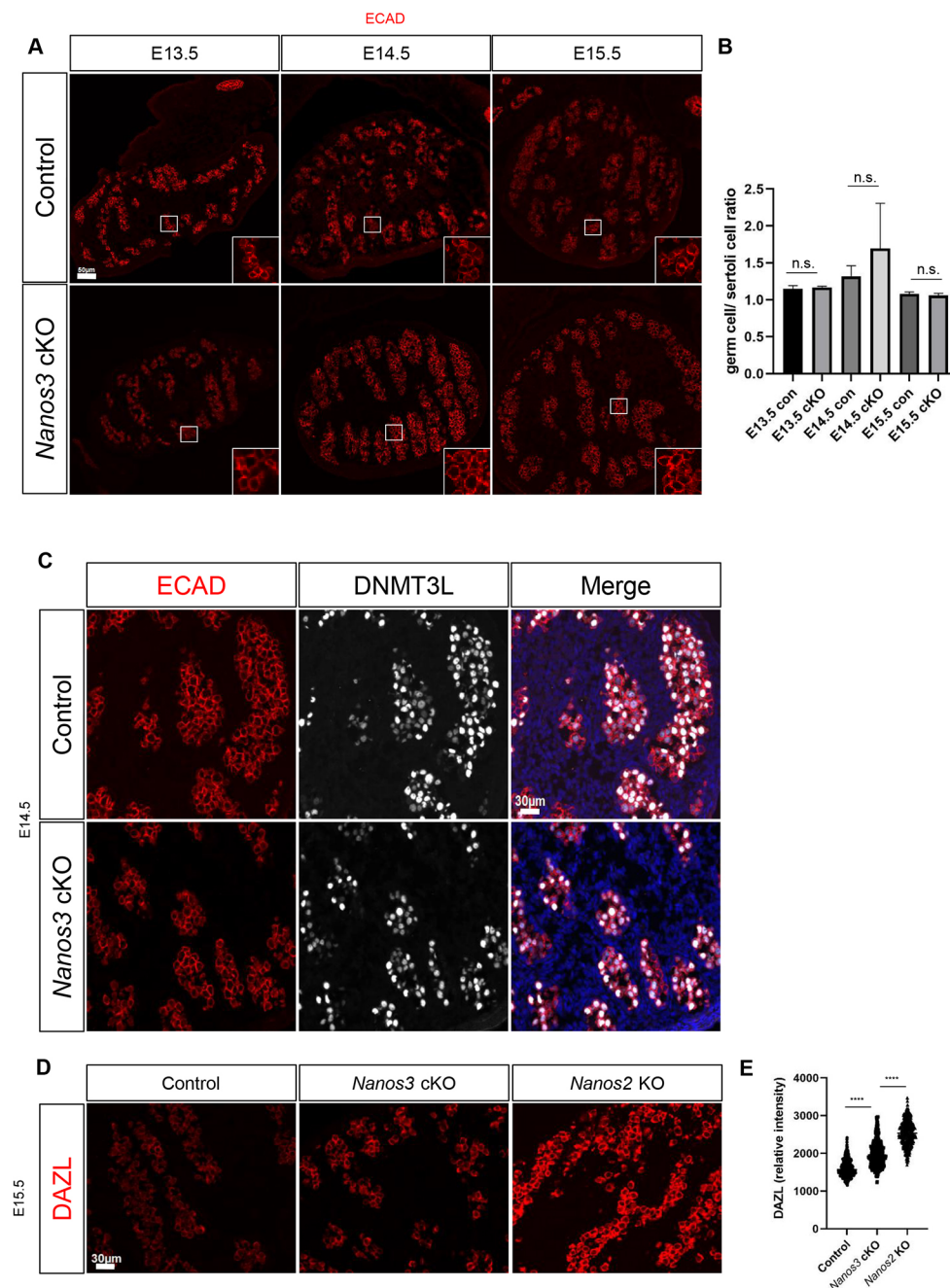
created via CRISPR/Cas9 technology, we attempted to clarify the roles and structural basis underlying the functional redundancy of NANOS proteins.

RESULTS

Male differentiation proceeds normally without NANOS3

Previous studies have revealed that NANOS3 is needed in PGCs to protect them from apoptosis as they migrate to the future gonad. However, its functions in later stages remain unclear. In males, its expression is downregulated after E13.5 (Suzuki et al., 2007), and it becomes expressed again during spermatogenesis after birth (Lolicato et al., 2008; Sada et al., 2009). As the amount of NANOS3 protein is low in embryonic male germ cells after NANOS2 becomes expressed (Suzuki et al., 2007), no studies have examined whether the complete loss of NANOS3 during this

interval affects germ cell development. Therefore, to address this, we created *Nanos3* conditional knockout mice. Pregnant *3xFlag-Nanos3^{flox/flox}/Nanos2^{+/mcherry}/Rosa CreERT²* mice were injected with tamoxifen at E11.5, and embryos were collected at embryonic day (E)13.5–E15.5. There was no FLAG-NANOS3 expression in E13.5 germ cells, confirming efficient Cre-mediated recombination (Fig. S1C). Cre-negative embryos were used as controls. At all time points, there was no difference in the number of germ cells between control and *Nanos3* cKO embryos (Fig. 1A,B). NANOS2 was normally expressed; therefore, expression of the male marker DNMT3L was observed, suggesting that the male pathway was successfully initiated (Fig. 1C, Fig. S1D). However, protein expression of the NANOS2 target, DAZL (Kato et al., 2016), was increased in the *Nanos3* cKO embryos compared with control embryos, even though NANOS2 was expressed (Fig. 1D,E).



Therefore, although the loss of NANOS3 resulted in germ cells having increased DAZL expression, this increase had no effect on male germ cell differentiation.

NANOS3 protects germ cells from apoptosis in the absence of NANOS2

NANOS3 becomes abnormally upregulated in *Nanos2* KO-germ cells. However, the function of this high NANOS3 expression was unclear because we were unable to compare it with the *Nanos2/3* dKO condition. Of note, in the presence of a NANOS2 ZF mutant, NANOS3 does not become upregulated and the cells exhibit a more severe fate than *Nanos2* KO cells, including germ cell death by E18.5 (Suzuki et al., 2016), suggesting that NANOS3 also exhibits slight functional redundancy in the absence of NANOS2. In

consideration of this, to assess the fate of germ cells in the absence of both NANOS proteins, we created *Nanos2/3* dKO mice. Pregnant *3xFlag-Nanos3^{flox/flox}/Nanos2^{mcherry/mcherry}/Rosa^{CreER^{T2}}* mice were injected with tamoxifen at E11.5, and embryos were collected at E13.5–E16.5. Cre-negative embryos were used as controls. At E13.5, there was no significant difference in the number of germ cells between dKO and control embryos, as we observed in the single *Nanos3* cKO (Figs 1A and 2A,B). However, few germ cells remained the following day at E14.5 and, by E15.5, the embryonic gonads were mostly devoid of germ cells (Fig. 2A,B), suggesting their rapid death. To check whether the cells were dying by apoptosis, testis sections were stained for cleaved PARP (cPARP). We compared dKO testes with wild-type and *Nanos2* KO testes at E14.5, but the number of cPARP signals in the dKO

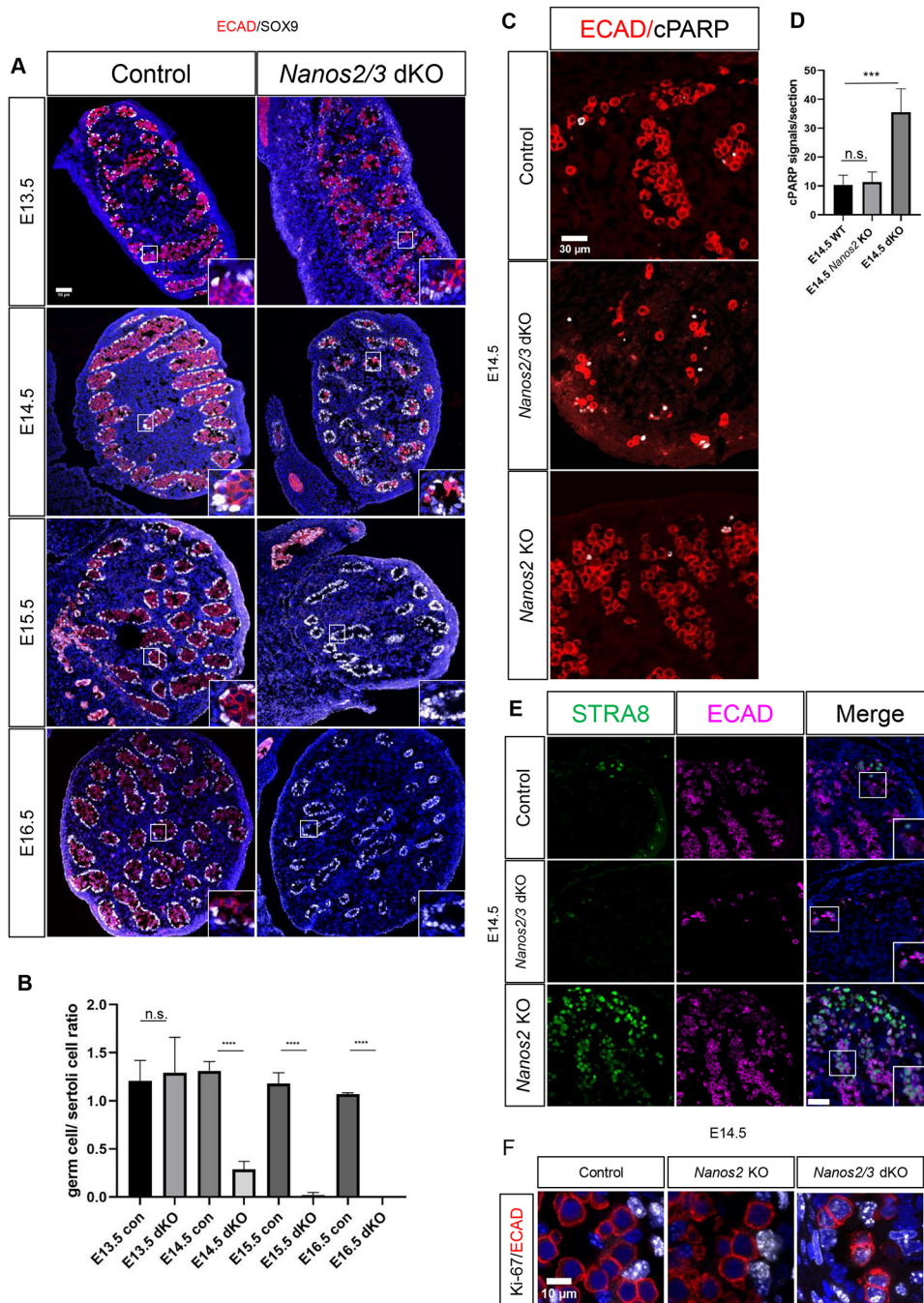


Fig. 2. Conditional double knockout of *Nanos2/3* leads to rapid germ cell death during the sexual differentiation stage.

(A) Sections of E13.5–E16.5 control and *Nanos2/3* dKO testes were stained with antibodies against E-cadherin (red) and SOX9 (white) to mark germ cells and Sertoli cells, respectively. DNA was stained with DAPI. Note the rapid loss of germ cells in the dKO between E13.5 and E14.5.

(B) Germ cell/Sertoli cell ratio in control and dKO testes (control and dKO E13.5–E16.5 $n=3$).

(C) E14.5 wild-type, *Nanos2* KO and dKO testis sections were stained with antibodies against cleaved PARP (white) and E-cadherin (red).

(D) Quantification of C-PARP signals in E14.5 wild-type, *Nanos2* KO and dKO testis sections.

(E) Sections of E14.5 control, *Nanos2* KO and *Nanos2/3* dKO testes were stained with antibodies against STRA8 (green) and E-cadherin (magenta).

(F) Sections of E14.5 control, *Nanos2* KO and *Nanos2/3* dKO testes were stained with antibodies against Ki-67 (white) and E-cadherin (red). Magnifications of boxed areas are shown in insets. Data are mean \pm s.d. *** $P < 0.0004$, **** $P < 0.0001$ (one-tailed unpaired Student's *t*-test). n.s., not significant. Scale bars: 50 μ m (A,E); 30 μ m (C); 10 μ m (F).

was higher, reflecting the more severe phenotype (Fig. 2C,D). Therefore, the dKO germ cells likely entered apoptosis soon after the E13.5 stage. *Nanos2* KO germ cells also died by apoptosis after E15.5, probably owing to the abnormal cell cycle regulation indicated by the upregulation of STRA8 and resumption of mitotic activity (Suzuki and Saga, 2008). To assess whether the dKO germ cells showed more severe cell cycle abnormality as expected by the rapid death, E14.5 testis sections were stained for STRA8 to mark meiosis and Ki-67 (Mki67) to mark the active cell cycle. In *Nanos2* KO mice, germ cells express STRA8, whereas its expression is suppressed in wild-type cells except in some cells near the mesonephros where the retinoic acid level is high. However, the dKO cells that were still alive had only weak or no expression of STRA8, being similar to the control (Fig. 2E). E14.5 dKO germ cells were positive for Ki-67, suggesting that the cell cycle was activated. This was in contrast to the control and *Nanos2* KO, in which the cell cycle is arrested, albeit only temporarily, at E14.5 – in the case of *Nanos2* KO in a large proportion of germ cells (Saba et al., 2014) (Fig. 2F). Therefore, in the absence of NANOS2, NANOS3 may suppress apoptosis by regulating genes related to the cell cycle.

NANOS2 is required for the maintenance of DND1 protein expression *in vivo*

One of the main mechanisms by which NANOS2 carries out its functions is by binding its partner DND1 and target RNA to form P-bodies. In *Dnd1* cKO germ cells, although no P-bodies are formed, the amount of NANOS2 protein is unchanged (Suzuki et al., 2016). In contrast, in our *Nanos2/3* dKO mice, the few remaining germ cells had lost the expression of DND1. DND1 was normally expressed at E13.5 (Fig. 3A), but was lost by E14.5 in *Nanos2/3* dKO germ cells (Fig. 3A). Reduced DND1 expression was also

observed in *Nanos2* KO, but not in *Nanos3* KO germ cells at E14.5 (Fig. S2A). As the *Dnd1* mRNA level does not differ between wild-type and *Nanos2* KO germ cells at E14.5 (Fig. S2B) (Butler et al., 2018; Shimada et al., 2020 preprint), DND1 may be stabilized by strong binding to NANOS2. To assess the protein stability of DND1, HEK293T cells were transfected with constructs for HA-DND1, FLAG-NANOS2 or NANOS3, and then treated with cycloheximide to inhibit translation. The cell lysates were collected at several time points after cycloheximide treatment and used for western blotting. There was no difference in DND1 protein when it was expressed alone or with NANOS2 or 3 (Fig. 3B, Fig. S2C). However, we found that NANOS2 protein expression decreased over time in the cultured cells. To examine whether the cell type and/or transient expression affected DND1 stability, the same experiment was performed using embryonic stem cells (ESCs) containing doxycycline-inducible FLAG-NANOS2 and HA-DND1 transgenes. However, similar to in HEK293T cells, DND1 protein was stable (Fig. 3C).

The NANOS2 ZF and N-terminal are both needed for male-type differentiation

Based on dKO analyses, the absence of both NANOS proteins causes the rapid loss of germ cells. In *Nanos2* KO germ cells, NANOS3 is upregulated, enabling the germ cells to survive for a longer period, but male-type differentiation does not occur. To understand the mechanism underlying the uneven functional redundancy, we looked closer at the structure of the proteins themselves. NANOS3 has a similar CCHC-CCHC ZF domain to NANOS2 and is able to localize to P-bodies with DND1 in *Nanos2* KO germ cells *in vivo* (Suzuki et al., 2012). Furthermore, the N-terminal is also relatively similar in amino acid sequence (Fig. 4A). Therefore, we hypothesized that these NANOS3

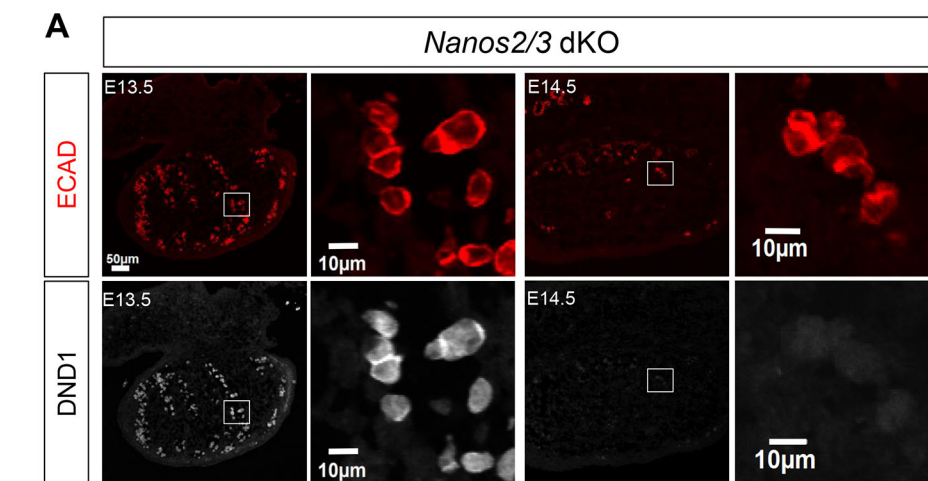
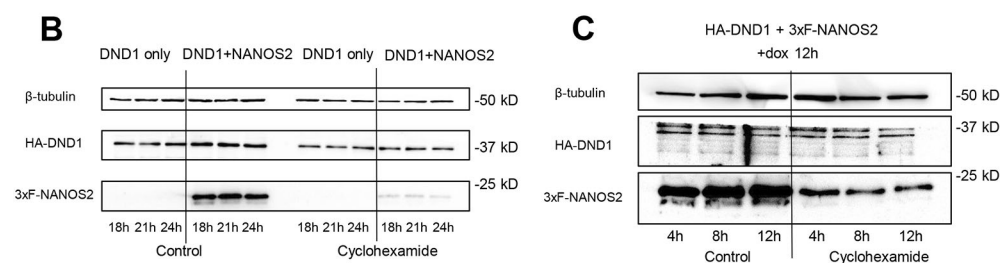


Fig. 3. Loss of NANOS causes the loss of DND1 *in vivo* but not in cultured cells. (A) Sections of testes from E13.5 and E14.5 *Nanos2/3* dKO embryos were stained with antibodies against DND1 (white) and E-cadherin (red). Enlarged images of boxed areas are shown on the right. (B) Western blotting of HEK293T cells expressing HA-DND1 alone or together with 3xFLAG-NANOS2 cultured with or without cycloheximide for the indicated times. β -Tubulin was used as a control. (C) Western blotting of inducible mouse ESCs cultured with or without cycloheximide for the indicated times. β -Tubulin was used as a control. Scale bars: 50 μ m; 10 μ m in enlarged images.



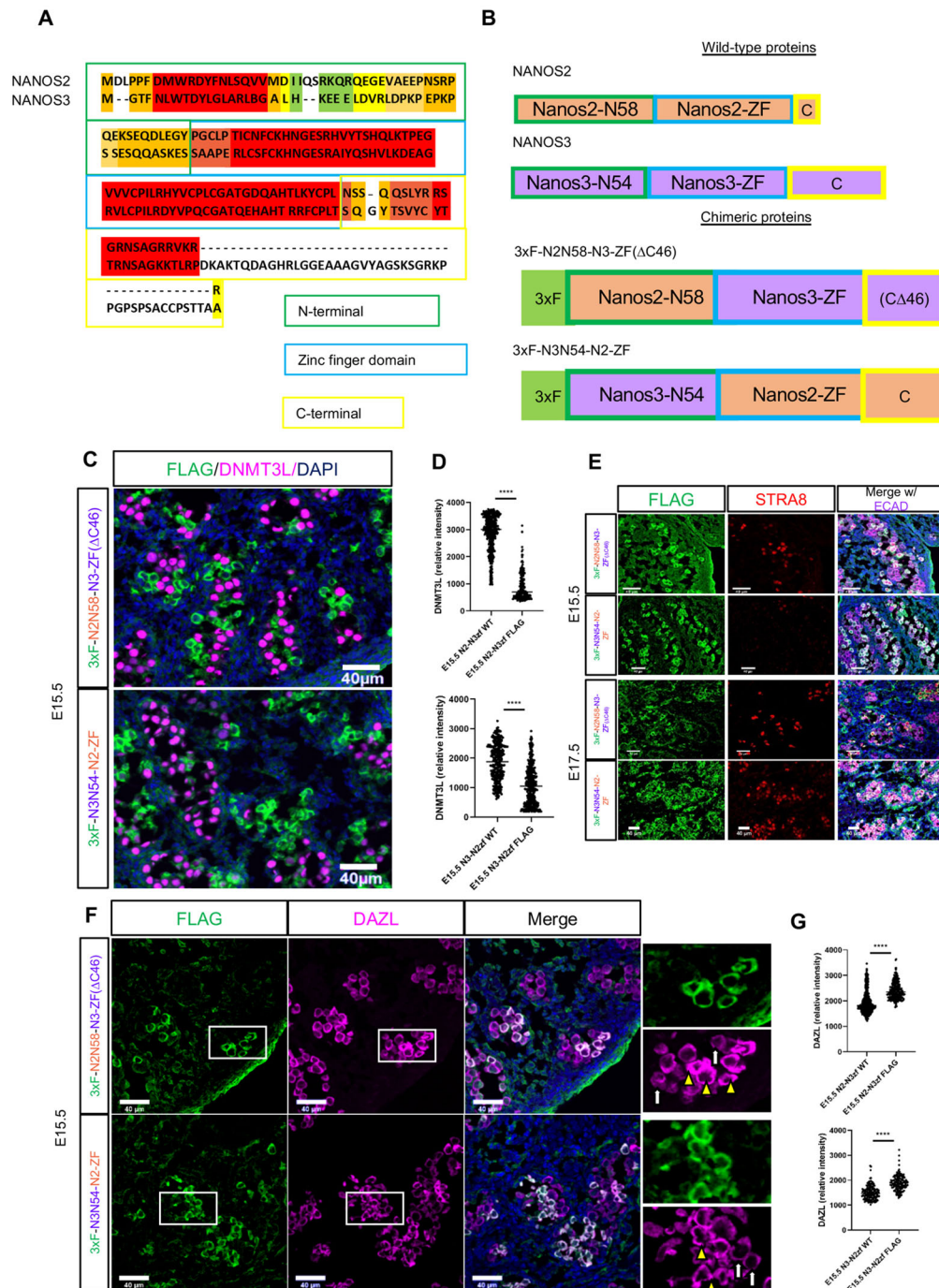


Fig. 4. Chimeric proteins failed to initiate the male pathway. (A) Comparison of NANOS2 and NANOS3 proteins by protein structural information using the T-coffee algorithm Expresso. Red indicates a high degree of structural similarity, yellow is moderate and green is low similarity. The key domains are outlined: the N terminal in green, ZF in blue and C terminal in yellow. Note that the NANOS3 C-terminal is 46 amino acids longer than the NANOS2 C-terminal. (B) Diagram of wild-type NANOS2 and NANOS3 protein domains (NANOS2 in orange, NANOS3 in purple) and of chimeric proteins made by interchanging NANOS2 and NANOS3 domains [top: 3xF-Nanos2N58-Nanos3-ZF(Δ C46), bottom: 3xF-Nanos3N54-Nanos2-ZF]. For 3xF-Nanos2N58-Nanos3-ZF(Δ C46), the last 46 amino acids of the NANOS3 C-terminal were removed. (C) Sections of E15.5 chimeric testes derived from ESCs containing 3xF-Nanos2N58-Nanos3-ZF(Δ C46) (top) or 3xF-Nanos3N54-Nanos2-ZF (bottom) were stained with antibodies against FLAG (green) and DNMT3L (magenta). DNA was labelled with DAPI (blue). (D) Quantification of DNMT3L immunostaining in 3xF-Nanos2N58-Nanos3-ZF(Δ C46) and 3xF-Nanos3N54-Nanos2-ZF chimeric testes. (E) Sections from E15.5 and E17.5 3xF-Nanos2N58-Nanos3-ZF(Δ C46) (top) or 3xF-Nanos3N54-Nanos2-ZF (bottom) testes were stained with antibodies against FLAG (green), STRA8 (red) and a germ cell marker (magenta). DNA was labelled with DAPI (blue). Compared with wild-type cells, FLAG-positive cells highly express STRA8 at E17.5. (F) Sections of E15.5 chimeric testes derived from ESCs containing 3xF-Nanos2N58-Nanos3-ZF(Δ C46) (top) or 3xF-Nanos3N54-Nanos2-ZF (bottom) were stained with antibodies against FLAG (green) and DAZL (magenta). DNA was labelled with DAPI (blue). Enlarged images of boxed areas are shown on the right. White arrows indicate wild-type cells and yellow arrowheads indicate mutant germ cells. (G) Quantification of DAZL immunostaining in 3xF-Nanos2N58-Nanos3-ZF(Δ C46) and 3xF-Nanos3N54-Nanos2-ZF chimeric testes. **** P <0.0001 (one-tailed unpaired Student's t -test). Scale bars: 40 μ m (C,F); 50 μ m (E).

domains themselves are able to replace the respective NANOS2 domains. For this purpose, we created two chimeric proteins with either the NANOS2 or NANOS3 ZF and full N-terminal (Fig. 4B). As NANOS3 has a longer C-terminal than NANOS2, this extra C-terminal sequence was deleted to examine whether it interferes with DND1 binding. As described in Materials and Methods, chimera mice expressing each chimeric protein were created via an ESC-mediated strategy (Shimada et al., 2019) and the resulting chimeric germ cells were analyzed for *Nanos2* KO phenotypes from E15.5.

Both 3xF-NANOS2-N58-NANOS3-ZF(Δ C46) and 3xF-NANOS3-N54-NANOS2-ZF chimeric proteins were expressed, and had a similar cytoplasmic localization pattern to endogenous NANOS2 (Fig. S3A). However, although neither mutant fully rescued the male differentiation pathway, as demonstrated by the lack of/weak DNMT3L expression, the quantification data suggest slight rescue via the 3xF-NANOS3-N54-NANOS2-ZF chimeric protein (Fig. 4C,D). The majority of wild-type (FLAG-negative) germ cells in the same testis had high DNMT3L expression. At E15.5, 3xF-NANOS2-N58-NANOS3-ZF(Δ C46)-expressing cells also expressed STRA8, which is normally absent but becomes upregulated in *Nanos2*-null germ cells. However, there was a delay in the upregulation of STRA8 in 3xF-NANOS3-N54-NANOS2-ZF-expressing cells. Most mutant cells were negative for STRA8 at E15.5, but by E17.5, STRA8 was upregulated (Fig. 4E), again suggesting slight rescue by the 3xF-NANOS3-N54-NANOS2-ZF chimeric protein. In either case, endogenous NANOS3 was still upregulated in all mutant germ cells according to immunostaining (Fig. S3B,C) and the NANOS2 target *Dazl* was not repressed in chimeric germ cells based on the increased DAZL protein expression (Fig. 4F,G).

Expression of DND1 is dependent on strong binding with the NANOS2 ZF domain

We found that both chimeric NANOS proteins failed to replace endogenous NANOS2 function. To investigate the reason, we further examined the properties of germ cells expressing chimeric proteins. Wild-type NANOS2 interacts with DND1 and localizes to P-bodies in male germ cells (Suzuki et al., 2016). We observed that DND1 was similarly localized to foci with both chimeric proteins (Fig. 5A). To assess the formation of P-bodies, we stained with an antibody against DDX6 (Rck; p54), a known P-body component that represses translation (Chu and Rana, 2006; Shimada et al., 2019). Chimeric germ cells expressing either 3xF-NANOS2-N58-NANOS3-ZF(Δ C46) or 3xF-NANOS3-N54-NANOS2-ZF had DDX6 foci, suggesting the formation of P-bodies (Fig. S4A,B). However, DND1 protein expression was reduced, especially in 3xF-NANOS2-N58-NANOS3-ZF(Δ C46)-expressing cells (Fig. 5A,B; Fig. S4A,B), similar to the reduction observed in *Nanos2* KO and dKO embryos. This suggests that DND1 expression is dependent on the presence of the NANOS2 ZF because the *Dnd1* mRNA level does not change in *Nanos2* KO (Fig. S2B). As there was limited DND1-chimeric protein localization, we considered that the binding of the proteins was affected.

To assess this possibility, we conducted several biochemical analyses. Using HEK293T cells, HA-DND1 was transfected with FLAG-tagged NANOS2 or NANOS3 to evaluate the binding strength *in vitro*. The amount of DND1 precipitated with NANOS3 was much lower than that for NANOS2, demonstrating the weaker binding strength of DND1 with the NANOS3 ZF (Fig. 5C). Next, the binding strength of the chimeric proteins with DND1 was assessed. 3xF-NANOS3-N54-NANOS2-ZF precipitated DND1 to

the same degree as NANOS2 and addition of the NANOS3 C-terminal had no effect on DND1 binding (Fig. 5C). However, 3xF-NANOS2-N58-NANOS3-ZF(Δ C46) was poorly expressed, suggesting that the NANOS3 C-terminal is needed for protein stabilization *in vitro* (Fig. 5C). As 3xF-NANOS2-N58-NANOS3-ZF(Δ C46) was expressed at levels similar to endogenous NANOS2 *in vivo* (Fig. S3A), other germ-cell specific factors may be involved in the stabilization of NANOS3 protein *in vivo*. Addition of the NANOS3 C-terminal restored 3xF-NANOS2-N58-NANOS3-ZF(Δ C46) expression in HEK293T cells (Fig. 5C), but it was still unable to precipitate more DND1. Thus, the NANOS2 ZF itself was reconfirmed as key for DND1 binding.

Specific NANOS2 amino acid configuration is required to carry out its activity

The chimeric protein expression analyses demonstrated that the ZF domain is responsible for the difference in binding ability of NANOS proteins to DND1. However, the T-Coffee algorithm Expresso (Armougom et al., 2006; Di Tommaso et al., 2011; Notredame et al., 2000; O'Sullivan et al., 2004; Poirrot et al., 2004), which aligns protein sequences based on protein structural information, indicated that the NANOS2 and 3 ZF amino acid sequences are markedly similar. It was previously reported that mutation of C61 and C96 to alanine in the CCHC-CCHC ZF motif of NANOS2 abolished DND1 interaction (Suzuki et al., 2016). Therefore, we examined whether the amino acids flanking the CCHC repeats that are different between NANOS2 and NANOS3 can explain the difference in DND1 binding strength. Point mutations were introduced to change the NANOS2 amino acid to the respective NANOS3 amino acid: I60L, N62S, Q78V, V87L, L98Q and Y111F (Fig. 6A). On immunoprecipitation with point mutants and DND1, all NANOS2 mutants had lower binding strength with DND1, with NANOS2-Y111F being the most reduced (Fig. 6B). As a single mutation was able to weaken NANOS2-DND1 binding, the opposite experiment was carried out and NANOS3 was mutated at L56I, S58N and F107Y, which equate to NANOS2 I60L, N62S and Y111F, respectively. The single mutation of F107Y was able to slightly increase the binding strength of NANOS3 for DND1, but all three mutations and even all six mutations together failed to further increase the amount of DND1 precipitated (Fig. 6C). Thus, although position Y111 may be important for DND1 binding, the entire NANOS2 ZF amino acid sequence is needed for correct DND1 interaction and RNA regulation. Using Phyre2 to create 3D models of the ZF domain (Kelley et al., 2015), we examined the differences between NANOS2 and NANOS3 (NANOS2 protein sequence: MGI 2676627; NANOS3 protein sequence: MGI 2675387) (Fig. S5). There was a slight difference in the side chain position between NANOS2 Y111 and NANOS3 F107 in relation to the CCHC side chains, which may affect binding.

The reduced binding between DND1 and the NANOS3 ZF explains why 3xF-NANOS2-N58-NANOS3-ZF(Δ C46) was unable to rescue male-type differentiation, but 3xF-NANOS3-N54-NANOS2-ZF had no decrease in binding strength and failed to rescue male-type differentiation as well. The NANOS2 N-terminal binds to the CNOT1 component of the CCR4-NOT complex *in vitro*, and previous studies revealed that full-length mouse NANOS3 is unable to directly bind CNOT1 (Suzuki et al., 2014, 2012). However, a previous study reported a CNOT interaction motif (NIM) containing conserved three amino acid residues (FWY) in the N-terminal of NANOS in several species (Bhandari et al., 2014). Human, *Xenopus* and zebrafish NANOS3 NIMs were able to

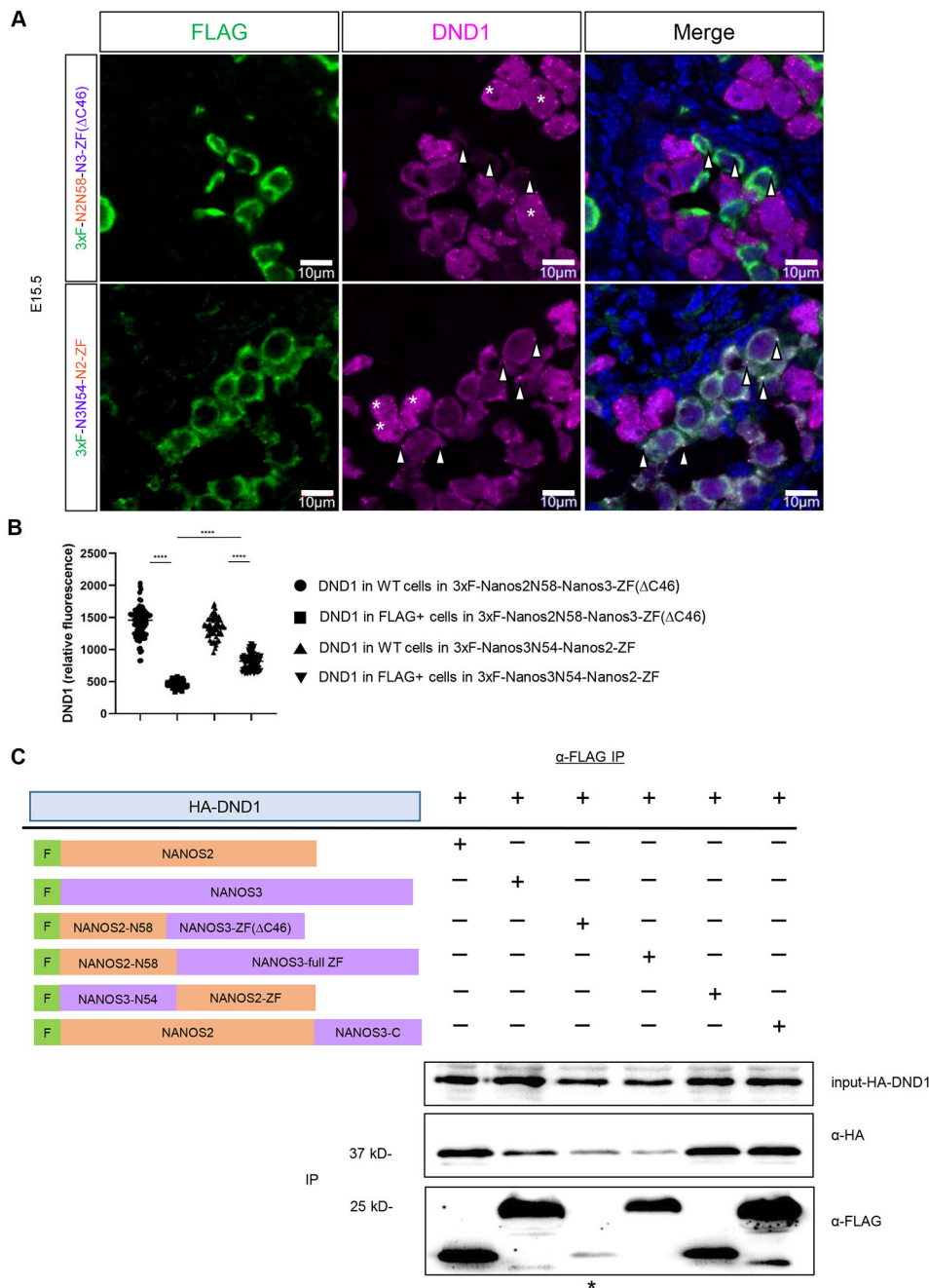


Fig. 5. DND1 strongly binds the NANOS2 ZF, but not the NANOS3 ZF. (A) Sections of testes from E15.5 3xF-Nanos2N58-Nanos3-ZF(ΔC46) (top) or 3xF-Nanos3N54-Nanos2-ZF (bottom) were stained with antibodies for FLAG (green) and DND1 (magenta). White arrowheads indicate merged DND1 and FLAG foci in chimeric germ cells. Asterisks indicate examples of wild-type cells. DNA was labelled with DAPI (blue). (B) Quantification of DND1 immunostaining in 3xF-Nanos2N58-Nanos3-ZF(ΔC46) and 3xF-Nanos3N54-Nanos2-ZF chimeric testes. **** $P < 0.0001$ (one-tailed unpaired Student's t -test). (C) Cultured HEK293T cells were transfected with HA-DND1 and FLAG-tagged NANOS2, NANOS3 or mutant proteins. Then, 48 h after transfection, cells were collected and used for immunoprecipitation with anti-FLAG beads. Co-precipitates were analyzed by western blotting with anti-FLAG and anti-HA antibodies. Asterisk indicates 3xF-NANOS2N58-NANOS3-ZF(ΔC46), which was hardly expressed in HEK293T cells. Scale bars: 10 μ m.

directly bind CNOT1 (Bhandari et al., 2014). As mouse NANOS3 also has this conserved NIM (Fig. 6D), a GST-pull-down experiment was conducted using both MBP-fused full-length NANOS3 and NANOS3 NIM to compare their ability to bind CNOT1. As previously reported (Suzuki et al., 2014), full-length mouse (m)NANOS3 cannot bind CNOT1, but both full-length mNANOS2 and the human (hu)NANOS3 NIM can (Fig. 6E). However, mNANOS3-NIM, despite being different from huNANOS3-NIM by only three amino acids (Fig. 6D), was unable to strongly bind CNOT1 compared with huNANOS3-NIM. To examine this further, we made a mutant mNANOS3 NIM, changing the second amino acid position from N to D, making it the same amino acid as in huNANOS3 and mNANOS2 NIMs. This mutant mNANOS3 NIM was still unable to bind CNOT1 strongly (Fig. 6F). Therefore, there is some other factor or modification involved.

The lack of rescue by 3xF-NANOS3-N54-NANOS2-ZF can be attributed to a reduced ability to bind CNOT1. This result is consistent with a previous study in which NANOS2 lacking the N-terminal failed to rescue *Nanos2*-null germ cells (Suzuki et al., 2012).

DISCUSSION

The long-standing question of why the structurally related NANOS proteins exhibit unequal functional redundancy during germ cell development has been partly answered by the current genetic and biochemical studies. There were two major questions: (1) Why is NANOS3 unable to rescue NANOS2 function even though its expression is strongly upregulated in the absence of NANOS2 and (2) is there any rescue event via the upregulated NANOS3? As shown in Fig. 2A, conditional double knockout of *Nanos2*

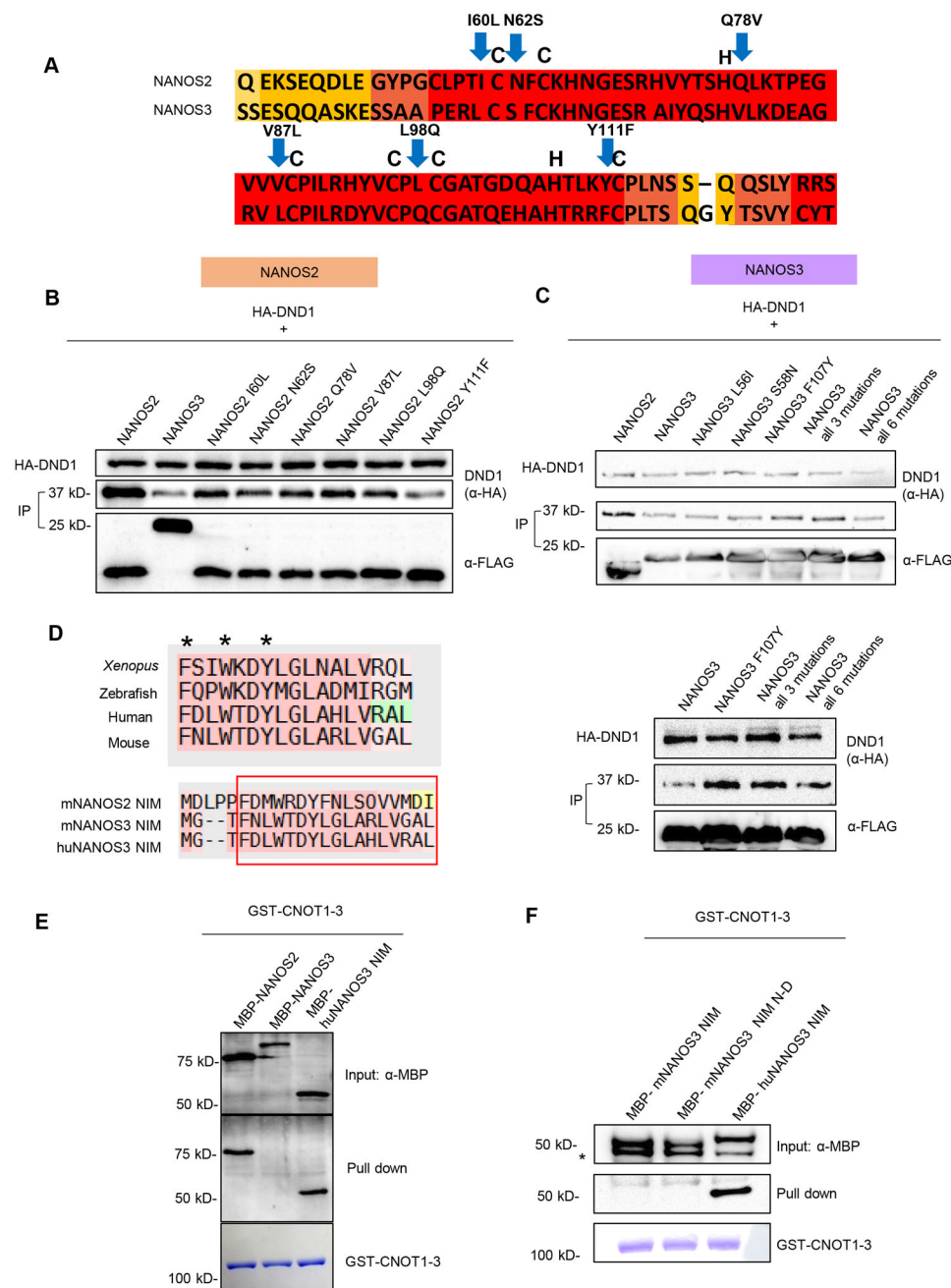


Fig. 6. Mouse NANOS3 cannot strongly bind DND1 or CNOT1. (A) CCHC-CCHC ZF domains of NANOS2 and NANOS3 are aligned and compared by protein structural information. Blue arrows indicate amino acids changed to make point mutants. (B,C) Cultured HEK293T cells were transfected with HA-DND1 and FLAG-tagged NANOS2, NANOS3, or NANOS2 or NANOS3 point mutants. Then, 48 h after transfection, cells were collected and used for immunoprecipitation with anti-FLAG beads. Co-precipitates were analyzed by western blotting with anti-FLAG and anti-HA antibodies. Representative blots of triplicate experiments are shown. (D) Comparison of NANOS3 NIM sequences for several species. Asterisks indicate amino acids reported to be required for CNOT1 interaction (FWY). The red box indicates the NIMs for mouse NANOS2 and NANOS3, and human NANOS3. (E) Each purified MBP-fusion protein was mixed with CNOT1-3-expressing *E. coli* lysate and then added to Glutathione Sepharose beads. The beads were boiled with SDS-PAGE loading buffer and run on acrylamide gels for CBB staining for CNOT1-3 or western blotting with anti-MBP. (F) mNANOS-NIM, mNANOS-NIM N-D and huNANOS3-NIM pulldown. Asterisk indicates background-expressed MBP tag, which was not pulled down.

and *Nanos3* led to the rapid loss of germ cells, demonstrating that NANOS3 functions in the absence of NANOS2 to protect germ cells from apoptotic cell death. On the other hand, conditional deletion of NANOS3 in the presence of NANOS2 did not cause any phenotype other than increased DAZL expression, but this increase had no effect on male differentiation. Thus, NANOS2 alone can protect against germ cell death and promote the male differentiation programme.

The combination of the different NANOS2 functional domains, N-terminal and ZF, is likely what enables full protein functionality and progression of male germ cell differentiation. As the NANOS3 and NANOS2 ZF domains have a similar structure, they were hypothesized to be able to replace each other. However, this was not the case, and the NANOS3 ZF only weakly bound DND1, as shown in Fig. 5C. To analyze the reason for this weaker binding, point-

mutation experiments were carried out, demonstrating that sequence specificity plays a large role in the binding of DND1. Binding strength was reduced the most by mutations next to the last cysteines (I60L, N62S and Y111F) of the CCHC repeats in the NANOS2 ZF domain. These cysteines may create a binding area for DND1, and the surrounding amino acids may need to be in a specific conformation to accommodate tight protein-protein/RNA interaction. As shown in Fig. 6B, NANOS2-Y111F had the greatest reduction in binding strength, which may have been caused by the small change in the amino acid side chain from tyrosine to phenylalanine. Using Phyre2 to create 3D models of the ZF domain, we examined differences between NANOS2 and 3. Mutation of NANOS2 Y111 to F111 caused the amino acid side chain orientation to shift to that observed in the NANOS3 model. Although it is currently unknown how and where DND1 binds, as

mutation of Y111 had strong negative effects, it may be involved in DND1 binding. Phosphorylation of tyrosine residues has been reported to affect protein binding and frequently occurs on binding interfaces, stabilizing protein complexes (Nishi et al., 2011). One of the RNA recognition motifs of human DND1 was recently crystallized (Kumari and Bhavesh, 2020 preprint), but how the NANOS2 ZF and mouse DND1 bind with mRNA remains undetermined.

The mechanism of how NANOS2 RNA targets are selected remains unknown. Currently, the only known mRNA target regulated during male-type differentiation is *Dazl* (Kato et al., 2016). Both chimeric mutants were likely unable to properly target and regulate RNA due to different reasons; the low DND1 binding strength [3xF-Nanos2N58-Nanos3ZF(Δ C46)] and inability to bind to the CCR4-NOT deadenylation complex correctly (3xF-Nanos3N54-Nanos2ZF). In the case of 3xF-Nanos3N54-Nanos2ZF germ cells, the phenotype was milder than that of 3xF-Nanos2N58-Nanos3ZF(Δ C46) germ cells in that DND1 expression was maintained (Fig. 5A), more cells expressed DNMT3L and STRA8 upregulation was delayed (Fig. 4C,E), probably due to the presence of the NANOS2 ZF. However, DND1 binding with the NANOS2 ZF alone is insufficient for the male pathway to proceed. The presence of DDX6 foci colocalized with DND1 signal, representing P-bodies, suggested that RNA was bound, but whether these P-bodies are similar to those formed in wild-type germ cells remains unknown. Therefore, even if RNAs were correctly targeted, P-body components, such as CCR4-NOT, may not be functioning correctly, as suggested by the increased protein expression of DAZL (Fig. 4F), the mRNA of which is targeted by NANOS2. This may have been because the mNANOS3 NIM cannot strongly bind CNOT1. The mNANOS3 NIM may be affected by other factors or folds to take a different protein structure, which thereby blocks its direct binding with CNOT1. It has been reported that mouse NANOS3 can directly bind CNOT8 *in vitro*, which may explain the inability to initiate male differentiation. CNOT1 is a scaffold protein and is able to interact with the deadenylases CNOT6, 6L, 7 and 8. On the other hand, CNOT8 competes with CNOT7 for binding to CNOT1, resulting in lower deadenylase activity (Suzuki et al., 2014). There may also be another factor that mediates NANOS3-CNOT-DND1 *in vivo*, but DND1 is not considered a partner protein of NANOS3. In cultured cells, NANOS3 does not localize with DND1 in P-bodies, but in *Nanos2* KO germ cells it does (Fig. S6A,B). Thus, protein interactions *in vivo* are different from in cultured cells and may be species-specific. For example, 3xF-NANOS2-N58-NANOS3-ZF(Δ C46) was normally expressed in chimeric mouse germ cells but was hardly expressed in HEK293T cells, suggesting that something is binding and/or stabilizing it *in vivo*. The *in vivo* functions of human NANOS3 are largely unknown, and this study suggests that they vary from those of mouse NANOS3.

Based on this study, the role of NANOS3 is to protect against cell death even after the germ cells enter the gonad. The sudden loss of germ cells between E13.5 and E14.5 observed in the dKO indicates the presence of a checkpoint for germ cell viability. In wild-type embryos, this timing is when there is a shift in the balance of NANOS2 and 3 expression, as well as events marking sex differentiation; female germ cells enter meiosis, whereas male germ cells arrest the cell cycle. There is a wave of apoptosis among PGCs at E13.5 (Coucouvanis et al., 1993). As NANOS3 mRNA expression stops after E13.5 in female germ cells, their successful meiotic entry may protect them from continued apoptosis. On the other hand, male germ cells begin to express NANOS2, which is

known to regulate the cell cycle. *Nanos2* expression and male differentiation were reported to mark an apoptosis-resistant state of germ cells, whereas the undifferentiated state was more prone to apoptosis (Nguyen et al., 2020). *Nanos2* KO male germ cells may not immediately die because NANOS3 is upregulated and they enter an abnormal cell cycle with STRA8 induction. As reported, waves of apoptosis are observed before meiotic entry in both males and females (Coucouvanis et al., 1993; Rucker et al., 2000), and the dKO germ cells expressed Ki-67, indicating failure of cell cycle arrest, the loss of germ cells in the dKO mice after E13.5 may have resulted from their inability to clear a cell cycle checkpoint and avoid apoptosis. The presence of either NANOS protein enables male germ cells to clear this hypothetical checkpoint, but only NANOS2 can promote the subsequent male pathway. The apparent superiority of NANOS2 likely resides in its structural properties, i.e. binding ability to CNOT1 and DND1, which is defective in NANOS3.

We speculate that NANOS3 cannot properly regulate NANOS2 targets, but it is still possible that it binds and regulates other mRNAs, such as those related to apoptosis (Suzuki et al., 2008), in the absence of NANOS2. Furthermore, NANOS3 expression may be related to the temporary cell cycle arrest and STRA8 upregulation observed in *Nanos2* KO at E14.5 because these phenotypes were not observed in the dKO. Determining how mRNA are successfully selected and regulated by RNA-binding proteins will further our understanding of how the male pathway is initiated. In conclusion, our study sheds light on the functional differences between NANOS2 and NANOS3 in germ cell development, providing an example of how two homologous proteins can have varying functions despite their similar structure.

MATERIALS AND METHODS

Mice

Mice were housed in a specific-pathogen-free animal care facility at the National Institute of Genetics (NIG). All experiments were approved by the NIG Institutional Animal Care and Use Committee. *Nanos2-mcherry*, *Nanos3 cKO* mice were generated by ESC-mediated homologous recombination. All mouse lines used in this study were of a mixed genetic background.

Production of *Nanos2-mCherry* mice

This line was derived from the *Nanos2 cKO* mouse line produced as follows: for the targeting vector construction, homologous arms and 3xFlag-*Nanos2* were prepared by PCR amplification from the mouse genome and 3x-Flag-*Nanos2*-cDNA construct previously reported (Suzuki and Saga, 2008), and were integrated into the DT-ApA/conditional KO FW vector containing the *loxP*, *Frt* and *Pgk*-neomycin cassette (targeting vector is available from RIKEN BRC #RDB18643). The mCherry cassette was integrated after the 3' *loxP* site just before the *Nanos2* 3' untranslated region (UTR). To facilitate homologous recombination, Cas9 target sites were selected using CRISPR direct (<http://crispr.dbcls.jp/>) and the target sequence (5'-GGGTTGCATCT-TGTTACATA-3') was integrated into the px330 Cas9 vector (Addgene plasmid #42230). The targeting vector and the Cas9 vector were transfected into TT2 ESCs, and the homologous recombinants were selected using 150 μ g/ml neomycin-containing medium. Correctly recombinant ESCs were screened using the following primer sets: *Nanos2*-cKO-L1 (5'-TATGTAACAAGATG-CAACC-3') and FLAG-R (5'-CACCGTCATGGTCTTTGTAGTCG-3') for 5' recombination, and CAT-pA-L4 (5'-CCTCTACAAATGTGGTATGGCTG-3') and N2-H2(H1?) (5'-CCTGCAACTCTGTAGACTAGGCTGGCC-3') for 3' recombination. These ESCs were aggregated with eight-cell embryos, and the blastocysts that formed the next day were transferred to foster mothers to generate chimeric mice. After confirming germline transmission, the neomycin cassette was removed by crossing with *Rosa-Flp* mice (Dymecki, 1996). To create *Nanos2^{mcherry}*, the mice were crossed with CAG-Cre mice to remove 3xFlag-*Nanos2*, as shown in Fig. S1A.

Production of Nanos3 conditional knockout mice

For targeting vector construction, the homologous arms and exon-1 part of *3xFlag-Nanos3* were prepared by PCR amplification from the mouse genome and *3xFlag-Nanos3* cDNA construct, and integrated into a vector containing two *loxP* sequences via the sequential infusion method (the targeting vector is available from RIKEN BRC #RDB18644). Two Cas9 target sites were selected using CRISPR direct (<http://crispr.dncls.jp/>), and each target sequence (5'-AAGGAAGTTGGAGCCAGGTT-3' and 5'-TC-TGTTGGCACTGGGTGCG-3') was integrated into the px330 Cas9 vector (Addgene plasmid #42230) containing the PGK-puromycin cassette. These vectors were transfected into ESCs established from the Rosa-CreERT mouse line using Lipofectamine 2000 (Invitrogen) and homologous recombinants were selected using 1 µg/ml puromycin-containing medium for the first 2 days. Correctly recombined ESCs were screened using the following primer sets: Nanos3-5'-UTR-F2 (5'-GGCATACTCTGCCCA-ACC-3') and FLAG-R (5'-CACCCTCATGGTCTTTGTAGTCG-3') for 5' recombination, and Lox-L1 (5'-GGACGTAACTCCTCTTCAGACC-3') and Nanos3-PC1 (5'-GACCCTCGCTGGGTTCACG-3') for 3' recombination. We obtained an ESC line that had a homozygously recombined *Nanos3-flox* allele. The ESC line was aggregated with eight-cell embryos to generate chimeric mice as described above. The schema for creating *Nanos3* cKO mice is shown in Fig. S1B.

Creation of conditional Nanos2/Nanos3 double knockout mice

A male *3xFlag-Nanos3^{flox/flox}/Rosa CreERT²* chimeric mouse was crossed with female *Nanos2^{mcherry/mcherry}* mice to produce conditional *Nanos2/Nanos3* double knockout offspring by injecting tamoxifen at E11.5 to induce Cre recombination. Using this mouse line, single conditional *Nanos3* knockout, single *Nanos2* knockout and double knockout mice were obtained. Genotypes were confirmed by PCR. *3xFlag-Nanos3^{flox/flox}/Nanos2^{+/mcherry}* mice negative for *Rosa CreERT²* were considered as controls. Testes for each genotype were collected at E13.5-E16.5, fixed in 4% PFA for 30 min, cryoprotected with sucrose, embedded in OCT compound and frozen at -80°C until analysis.

Creation of mutant NANOS protein-expressing chimeric mice

To evaluate the functional domains of NANOS proteins, mutant constructs were created by interchanging the DNA domains encoding the N-terminal and ZF of NANOS2 and NANOS3. NANOS3 has a longer C-terminal than NANOS2. The extra C-terminal sequence (46 amino acids) was deleted such that it was the same length as that of NANOS2. The final two DNA constructs, 3xF-Nanos2N58-Nanos3ZF(ΔC46) and 3xF-Nanos3N54-Nanos2ZF, were knocked into the *Nanos2* locus in mouse ESCs using CRISPR/Cas9 gene editing (Cong et al., 2013). Homozygously mutated ESCs for each construct were aggregated with eight-cell mouse embryos to create chimeras. Chimeric testes were collected from E15.5, prepared as above, and immunohistochemically analyzed for male germ cell differentiation.

Immunohistochemistry

Frozen samples were cut into 5-µm-thick slices and placed on coated glass slides. The slides were autoclaved at 105°C for 15 min for antigen retrieval in Target Retrieval Solution (Dako). After rinsing with phosphate-buffered saline (PBS), the slides were blocked with 3% skim milk in PBS with 0.1% Tween® (PBST) for 1 h at room temperature (RT). The slides were then incubated with the following antibodies in Can Get Signal (Toyobo) at 4°C overnight: anti-FLAG-HRP (Sigma-Aldrich, 1/1000, #A8592), anti-DND1 (gift from Dr Suzuki, Yokohama National University, 1/1000), anti-Rck/p54 (DDX6; MBL, 1/300), anti-Ki-67 (Thermo Fisher Scientific, 1/200, #RM-9106-S0), anti-STRA8 (gift from Dr Ishiguro, Kumamoto University, 1/3000), anti-DNMT3L (gift from Dr Yamanaka, Kyoto University, 1/500), anti-E-Cadherin (R&D Systems, 1/500, #AF748), anti-NANOS3 [Suzuki et al. (2007), 1/300], anti-DAZL (Abcam, 1/300, #ab34139), anti-cleaved PARP (Cell Signaling Technologies, 1/300, #9548) and anti-SOX9 (Santa Cruz Biotechnology, 1/300, #sc-20095). The slides were washed three times in PBST and incubated with the respective secondary antibodies conjugated with Alexa Fluor 488, 594 or 647 (Invitrogen A32814, A32754, A32744, A32795, A21450; 1/250) in PBST for 90 min at RT. After washing with PBST and PBS, the slides were stained with

4',6-diamidino-2-phenylindole (DAPI) and coverslips were mounted. For anti-FLAG-HRP staining, slides were incubated for 10 min in 3% hydrogen peroxide/PBS to stop endogenous peroxidase activity before autoclaving. To detect HRP, the TSA kit (Perkin Elmer) was used following the manufacturer's instructions. Slides were imaged using an Olympus FV1200 confocal microscope. The obtained fluorescence images were analyzed using the ImageJ package Fiji (Schindelin et al., 2012).

Western blotting

Samples were boiled in 2× sample buffer for 5 min and run on gels for sodium dodecyl sulphate-polyacrylamide gel electrophoresis (SDS-PAGE). They were then transferred to PVDF (Immobilon) membranes. Membranes were blocked in 5% skim milk/PBST for 1 h at RT. They were then incubated with the following primary antibodies overnight at 4°C: mouse anti-FLAG-HRP (Sigma-Aldrich, 1/10000, #A8592), rabbit anti-HA (Santa Cruz Biotechnology, 1/2000, #sc-805) and mouse anti-β-tubulin (Sigma-Aldrich, 1/4000, #T4026). After washing three times with PBST, membranes were incubated with HRP-conjugated secondary antibodies for 1 h at RT. Protein bands were visualized using SuperSignal™ West Femto Maximum Sensitivity Substrate (Thermo Fisher Scientific).

Protein stability analysis

Protein stability was assessed using cultured HEK293T cells (ATCC) (transfected with expression vectors for HA-DND1 alone or together with 3xF-NANOS2, -NANOS3, or -NANOS2-3C) and doxycycline-inducible ESCs. ESCs were established using the PiggyBac system (Yamane et al., 2018) and expressed 3xF-NANOS2-t2a-HA-DND1 upon doxycycline addition. Cells were cultured with or without cycloheximide, and cell lysates were used for western blotting with anti-HA (Santa Cruz Biotechnology, #sc-805, 1/2000), anti-FLAG-HRP (Sigma-Aldrich, #A8592, 1/10000) and anti-β-tubulin (Sigma-Aldrich, #T4026, 1/4000).

DND1-NANOS binding analysis

NANOS-DND1 binding was examined using cultured HEK293T cells (ATCC) (transfected with expression vectors for HA-DND1 and FLAG-NANOS2, -NANOS3 or the mutant proteins used in the chimera analysis). Cell lysates were used for immunoprecipitation with anti-FLAG (M2) (Sigma-Aldrich) agarose beads 48 h after transfection. Co-precipitated DND1 was evaluated by western blotting with anti-HA (Santa Cruz Biotechnology, 1/2000, #sc-805) and anti-FLAG-HRP (Sigma-Aldrich, 1/10,000, #A8592) antibodies. NANOS single point mutants were created using site-directed mutagenesis (Laible and Boonrod, 2009). HEK293T cells were transfected with expression vectors for HA-DND1 and 3xF-NANOS2 single point mutants (I60L, N62S, Q78V, V87L, L98Q or Y111F) or NANOS3 point mutants (L56I, S58N, F107Y) (all three mutations or all six mutations) using polyethylenimine method. Then, 48 h after transfection, cells were collected and lysates were used for immunoprecipitation, as above.

Glutathione-S-transferase (GST) pull-down for CNOT1-NANOS direct binding

MBP-fused full-length mouse NANOS2, NANOS3 and GST-CNOT1-3-expressing *Escherichia coli* were generously provided by Dr Suzuki (Suzuki et al., 2014). CNOT1-3 refers to the C-terminal portion of the CNOT1 protein, which is where NANOS2 reportedly binds (Suzuki et al., 2014). To create MBP-fusion human NANOS3 NIM (huNANOS3-NIM) and MBP-fusion mouse NANOS3 NIM (mNANOS3-NIM) proteins, oligonucleotides encoding the respective NIM domains were annealed and ligated into the pMALc2 vector (New England Biolabs, #E8200) (Bhandari et al., 2014). BL21(DE3) *E. coli* were transformed with each pMAL construct and resulting clones were confirmed by DNA sequencing. MBP-fusion protein expression was induced by the addition of IPTG following the manufacturer's instructions. MBP-NANOS2, MBP-NANOS3, MBP-mNANOS3-NIM, MBP-mNANOS3-NIM N-D and MBP-huNANOS3-NIM were affinity purified using amylose resin (New England Biolabs), and proteins were confirmed by western blotting with anti-MBP (New England Biolabs, 1/10,000, E8032S). GST-CNOT1-3 protein expression was induced following previously reported methods (Suzuki et al., 2014).

Each purified MBP-fusion protein was mixed with GST-CNOT1-3-expressing *E. coli* lysate and rotated at 4°C for 1.5 h. Protein mixtures were added to Glutathione Sepharose 4B beads (Amersham Biosciences) and rotated at 4°C for 2 h. Beads were washed and boiled with loading buffer for subsequent SDS-PAGE and western blotting. CNOT1-3 expression was confirmed by Coomassie Brilliant Blue (CBB) staining.

Statistical analysis

To quantify immunofluorescence, signals on testis sections stained on the same slide from three embryos for each genotype were measured in Fiji. Cell counts were also similarly performed using Fiji. Significant differences between genotypes were assessed using the unpaired Student's *t*-test with Graphpad Prism 8. The error bars indicate s.d. A *P*-value of <0.05 was considered significant.

Acknowledgements

We greatly appreciate the Mouse Unit at the National Institute of Genetics for helping to create the mouse lines and chimeric mice. We also thank Dr Suzuki for providing anti-DND1 and the protein constructs, Dr Ishiguro for anti-STRA8 and Dr Yamanaka for anti-DNMT3L.

Competing interests

The authors declare no competing or financial interests.

Author contributions

Conceptualization: D.W., Y.S.; Methodology: D.W., M.K., Y.S.; Validation: D.W.; Formal analysis: D.W.; Investigation: D.W.; Resources: M.K., Y.S.; Writing - original draft: D.W., Y.S.; Writing - review & editing: D.W., Y.S.; Visualization: D.W., Y.S.; Supervision: Y.S.; Project administration: Y.S.; Funding acquisition: Y.S.

Funding

This work was supported by the Japan Society for the Promotion of Science KAKENHI grant numbers 16H06279 and 17H06166.

Data availability

Single-cell RNA-seq data have been deposited into the DNA Data Bank of Japan (DDBJ) under accession number DRA011172.

Supplementary information

Supplementary information available online at <https://dev.biologists.org/lookup/doi/10.1242/dev.191916.supplemental>

Peer review history

The peer review history is available online at <https://dev.biologists.org/lookup/doi/10.1242/dev.191916.reviewer-comments.pdf>

References

- Aizer, A., Brody, Y., Ler, L. W., Sonenberg, N., Singer, R. H. and Shav-Tal, Y. (2008). The dynamics of mammalian P body transport, assembly, and disassembly in vivo. *Mol. Biol. Cell* **19**, 4154-4166. doi:10.1091/mbc.e08-05-0513
- Armougom, F., Moretti, S., Poirot, O., Audic, S., Dumas, P., Schaeli, B., Kedue, V. and Notredame, C. (2006). Expresso: automatic incorporation of structural information in multiple sequence alignments using 3D-Coffee. *Nucleic Acids Res.* **34**, W604-W608. doi:10.1093/nar/gkl092
- Bhandari, D., Raisch, T., Weichenrieder, O., Jonas, S. and Izaurralde, E. (2014). Structural basis for the Nanos-mediated recruitment of the CCR4-NOT complex and translational repression. *Genes Dev.* **28**, 888-901. doi:10.1101/gad.237289.113
- Butler, A., Hoffman, P., Smibert, P., Papalexi, E. and Satija, R. (2018). Integrating single-cell transcriptomic data across different conditions, technologies, and species. *Nat. Biotechnol.* **36**, 411-420. doi:10.1038/nbt.4096
- Chu, C.-Y. and Rana, T. M. (2006). Translation repression in human cells by microRNA-induced gene silencing requires RCK/p54. *PLoS Biol.* **4**, e210. doi:10.1371/journal.pbio.0040210
- Cong, L., Ran, F. A., Cox, D., Lin, S., Barretto, R., Habib, N., Hsu, P. D., Wu, X., Jiang, W., Marraffini, L. A. et al. (2013). Multiplex genome engineering using CRISPR/Cas systems. *Science* **339**, 819-823. doi:10.1126/science.1231143
- Coucouvanis, E. C., Sherwood, S. W., Carswell-Crumpton, C., Spack, E. G. and Jones, P. P. (1993). Evidence that the mechanism of prenatal germ cell death in the mouse is apoptosis. *Exp. Cell Res.* **209**, 238-247. doi:10.1006/excr.1993.1307
- Decker, C. J. and Parker, R. (2012). P-bodies and stress granules: possible roles in the control of translation and mRNA degradation. *Cold Spring Harb. Perspect. Biol.* **4**, a012286. doi:10.1101/cshperspect.a012286
- Di Tommaso, P., Moretti, S., Xenarios, I., Orobitt, M., Montanyola, A., Chang, J.-M., Taly, J.-F. and Notredame, C. (2011). T-Coffee: a web server for the multiple sequence alignment of protein and RNA sequences using structural information and homology extension. *Nucleic Acids Res.* **39**, W13-W17. doi:10.1093/nar/gkr245
- Dymecki, S. M. (1996). Flp recombinase promotes site-specific DNA recombination in embryonic stem cells and transgenic mice. *Proc. Natl. Acad. Sci. USA* **93**, 6191-6196. doi:10.1073/pnas.93.12.6191
- Eulalio, A., Behm-Ansmant, I. and Izaurralde, E. (2007). P bodies: at the crossroads of post-transcriptional pathways. *Nat. Rev. Mol. Cell Biol.* **8**, 9-22. doi:10.1038/nrm2080
- Gross-Thebing, T. and Raz, E. (2020). Dead end and Detour: the function of the RNA-binding protein Dnd in posttranscriptional regulation in the germline. *Curr. Top. Dev. Biol.* **140**, 181-208. doi:10.1016/bs.ctdb.2019.12.003
- Haraguchi, S., Tsuda, M., Kitajima, S., Sasaoka, Y., Nomura-Kitabayashi, A., Kurokawa, K. and Saga, Y. (2003). nanos1: a mouse nanos gene expressed in the central nervous system is dispensable for normal development. *Mech. Dev.* **120**, 721-731. doi:10.1016/S0925-4773(03)00043-1
- Kato, Y., Katsuki, T., Kokubo, H., Masuda, A. and Saga, Y. (2016). Dazl is a target RNA suppressed by mammalian NANOS2 in sexually differentiating male germ cells. *Nat. Commun.* **7**, 11272. doi:10.1038/ncomms11272
- Kedersha, N., Stoecklin, G., Ayodele, M., Yacono, P., Lykke-Andersen, J., Fritzler, M. J., Scheuner, D., Kaufman, R. J., Golan, D. E. and Anderson, P. (2005). Stress granules and processing bodies are dynamically linked sites of mRNP remodeling. *J. Cell Biol.* **169**, 871-884. doi:10.1083/jcb.200502088
- Kelley, L. A., Mezulis, S., Yates, C. M., Wass, M. N. and Sternberg, M. J. E. (2015). The Pyre2 web portal for protein modeling, prediction and analysis. *Nat. Protoc.* **10**, 845-858. doi:10.1038/nprot.2015.053
- Kumari, P. and Bhavesh, N. S. (2020). Human DND1-RRM2 forms a non-canonical domain swapped dimer. *bioRxiv* 2020.03.05.978023. doi:10.1101/2020.03.05.978023
- Laible, M. and Boonrod, K. (2009). Homemade site directed mutagenesis of whole plasmids. *J. Vis. Exp.* **27**, e1135. doi:10.3791/1135
- Licatalosi, D. D. (2016). Roles of RNA-binding proteins and post-transcriptional regulation in driving male germ cell development in the mouse. In *RNA Processing: Disease and Genome-Wide Probing, Advances in Experimental Medicine and Biology* (ed. G. W. Yeo), pp. 123-151. Cham: Springer International Publishing.
- Lolicato, F., Marino, R., Paronetto, M. P., Pellegrini, M., Dolci, S., Geremia, R. and Grimaldi, P. (2008). Potential role of Nanos3 in maintaining the undifferentiated spermatogonia population. *Dev. Biol.* **313**, 725-738. doi:10.1016/j.ydbio.2007.11.011
- Nguyen, D.H., Soygur, B., Peng, S. P., Malki, S., Hu, G. and Laird, D. J. (2020). Apoptosis in the fetal testis eliminates developmentally defective germ cell clones. *Nat. Cell Biol.* **22**, 1423-1435. doi:10.1038/s41556-020-00603-8
- Nishi, H., Hashimoto, K. and Panchenko, A. R. (2011). Phosphorylation in protein-protein binding: effect on stability and function. *Structure* **19**, 1807-1815. doi:10.1016/j.str.2011.09.021
- Notredame, C., Higgins, D. G. and Hering, J. (2000). T-coffee: a novel method for fast and accurate multiple sequence alignment 1 Edited by J. Thornton. *J. Mol. Biol.* **302**, 205-217. doi:10.1006/jmbi.2000.4042
- O'Sullivan, O., Suhre, K., Abergel, C., Higgins, D. G. and Notredame, C. (2004). 3DCoffee: combining protein sequences and structures within multiple sequence alignments. *J. Mol. Biol.* **340**, 385-395. doi:10.1016/j.jmb.2004.04.058
- Poirot, O., Suhre, K., Abergel, C., O'Toole, E. and Notredame, C. (2004). 3DCoffee@igs: a web server for combining sequences and structures into a multiple sequence alignment. *Nucleic Acids Res.* **32**, W37-W40. doi:10.1093/nar/gkh382
- Rucker, E. B., Dierisseau, P., Wagner, K.-U., Garrett, L., Wynshaw-Boris, A., Flaws, J. A. and Hennighausen, L. (2000). Bcl-x and Bax regulate mouse primordial germ cell survival and apoptosis during embryogenesis. *Mol. Endocrinol.* **14**, 1038-1052. doi:10.1210/mend.14.7.0465
- Saba, R., Kato, Y. and Saga, Y. (2014). NANOS2 promotes male germ cell development independent of meiosis suppression. *Dev. Biol.* **385**, 32-40. doi:10.1016/j.ydbio.2013.10.018
- Sada, A., Suzuki, A., Suzuki, H. and Saga, Y. (2009). The RNA-binding protein NANOS2 is required to maintain murine spermatogonial stem cells. *Science* **325**, 1394-1398. doi:10.1126/science.1172645
- Schindelin, J., Arganda-Carreras, I., Frise, E., Kaynig, V., Longair, M., Pietzsch, T., Preibisch, S., Rueden, C., Saalfeld, S., Schmid, B. et al. (2012). Fiji: an open-source platform for biological-image analysis. *Nat. Methods* **9**, 676-682. doi:10.1038/nmeth.2019
- Shimada, R., Kiso, M. and Saga, Y. (2019). ES-mediated chimera analysis revealed requirement of DDX6 for NANOS2 localization and function in mouse germ cells. *Sci. Rep.* **9**, 515. doi:10.1038/s41598-018-36502-0
- Shimada, R., Koike, H., Hirano, T. and Saga, Y. (2020). NANOS2 suppresses the cell cycle by repressing mTORC1 activators in embryonic male germ cells. *bioRxiv* 2020.09.23.310912. doi:10.1101/2020.09.23.310912
- Stoecklin, G. and Kedersha, N. (2013). Relationship of GW/P-bodies with stress granules. In *Ten Years of Progress in GW/P Body Research, Advances in Experimental Medicine and Biology* (ed. E. K. L. Chan and M. J. Fritzler), pp. 197-211. New York, NY: Springer.
- Suzuki, A. and Saga, Y. (2008). Nanos2 suppresses meiosis and promotes male germ cell differentiation. *Genes Dev.* **22**, 430-435. doi:10.1101/gad.1612708

- Suzuki, A., Tsuda, M. and Saga, Y.** (2007). Functional redundancy among Nanos proteins and a distinct role of Nanos2 during male germ cell development. *Development* **134**, 77-83. doi:10.1242/dev.02697
- Suzuki, H., Tsuda, M., Kiso, M. and Saga, Y.** (2008). Nanos3 maintains the germ cell lineage in the mouse by suppressing both Bax-dependent and -independent apoptotic pathways. *Dev. Biol.* **318**, 133-142. doi:10.1016/j.ydbio.2008.03.020
- Suzuki, A., Saba, R., Miyoshi, K., Morita, Y. and Saga, Y.** (2012). Interaction between NANOS2 and the CCR4-NOT deadenylation complex is essential for male germ cell development in mouse. *PLoS ONE* **7**, e33558. doi:10.1371/journal.pone.0033558
- Suzuki, A., Niimi, Y. and Saga, Y.** (2014). Interaction of NANOS2 and NANOS3 with different components of the CNOT complex may contribute to the functional differences in mouse male germ cells. *Biol. Open* **3**, 1207-1216. doi:10.1242/bio.20149308
- Suzuki, A., Niimi, Y., Shinmyozu, K., Zhou, Z., Kiso, M. and Saga, Y.** (2016). Dead end1 is an essential partner of NANOS2 for selective binding of target RNAs in male germ cell development. *EMBO Rep.* **17**, 37-46. doi:10.15252/embr.201540828
- Tsuda, M.** (2003). Conserved role of nanos proteins in germ cell development. *Science* **301**, 1239-1241. doi:10.1126/science.1085222
- Yamane, M., Ohtsuka, S., Matsuura, K., Nakamura, A. and Niwa, H.** (2018). Overlapping functions of Krüppel-like factor family members: targeting multiple transcription factors to maintain the naïve pluripotency of mouse embryonic stem cells. *Development* **145**, dev162404. doi:10.1242/dev.162404